

Supporting Information for:

Characterization of two modes in a dielectric barrier discharge probe by optical emission spectroscopy and time-of-flight mass spectrometry

A. Bierstedt^a, U. Panne^{a,b}, K. Rurack^a, J. Riedel^a

a BAM, Federal Institute for Materials Research and Testing, Richard-Willstätter-Straße 11,
12489 Berlin, Germany

b Humboldt-Universität zu Berlin, Department of Chemistry, Brook-Taylor-Straße 2, 12489
Berlin, Germany

Corresponding author: Jens Riedel, Email: Jens.Riedel@bam.de, Phone: +49 30 8104-1162,
Fax: +49 30 8104-1167

Keywords: Dual mode, Dielectric barrier discharge, Ambient desorption/ionization mass
spectrometry, Emission spectroscopy, Ionization

Blank spectra analysis

Typically in ambient plasma-based ionization sources protonated water clusters are accompanied by a number of different molecular ions that can promote ionization *via* charge-transfer reactions. Fig. S1 depicts a steady-state signal using a previously described homebuilt inlet suitable for a rather direct interrogation of the reactive species present in the DBD source gas stream.¹ Briefly, it consists of a capped hollow cylinder (i.d. 3 mm) with a central pinhole (300 μm). The inlet was held at room temperature and its electric potential was floating. All measurements were performed under single reflectron geometry.

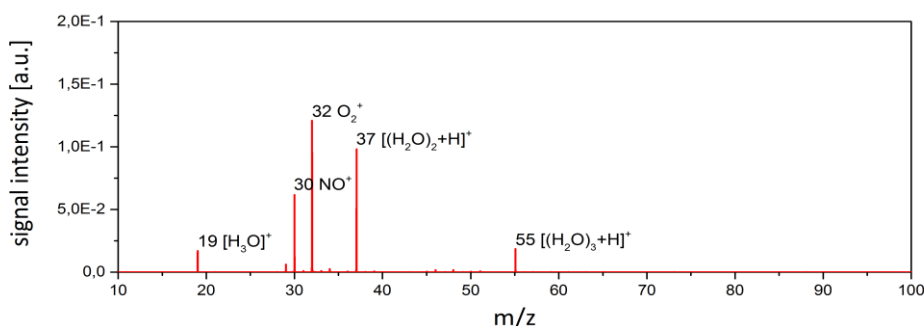


Fig. S1: MS background spectra using API-HTOF system equipped with a homebuilt atmospheric pressure inlet. The main features are protonated water clusters $[(\text{H}_2\text{O})_n\text{H}]^+$ accompanied by additional charge-transfer reagent-ions such as NO^+ and O_2^+ .

In addition to already described series of protonated water clusters, signals at m/z 30 and 32 indicate the known formation of NO^+ and O_2^+ in plasma-based ion sources, such as flowing atmospheric pressure afterglow (FAPA) and the low-temperature plasma (LTP) probe.^{1–3} Additional ionic species in lower abundance were identified to be m/z 46 NO_2^+ , m/z 48 O_3^+ , m/z 33 O_2H^+ and m/z 29 N_2H^+ .⁴

Identification of NH_4^+ using high-resolution TOFMS

The mass spectrometer used throughout these studies was capable of providing high resolution m/z values. Therefore mass differences between selected odd and even numbered clusters were calculated and compared to the theoretical mass differences for the formation of either ammonium water adducts or formation of radical water clusters. Experimental mass difference was 0.98474 u for signals with the highest abundance, in this case $[(\text{H}_2\text{O})_5\text{H}]^+$ and $[(\text{NH}_3)(\text{H}_2\text{O})_4\text{H}]^+$, and 0.98145 u for a selected pair of water clusters in the higher mass region, $[(\text{H}_2\text{O})_{25}\text{H}]^+$ and $[(\text{NH}_3)(\text{H}_2\text{O})_{24}\text{H}]^+$. Theoretical calculated mass difference for H_3O^+ and NH_4^+ is 0.9843 u, whereas the mass difference for H_3O^+ and H_2O^+ is 1.008 u. These observations corroborate the identity of ammonium adducts.

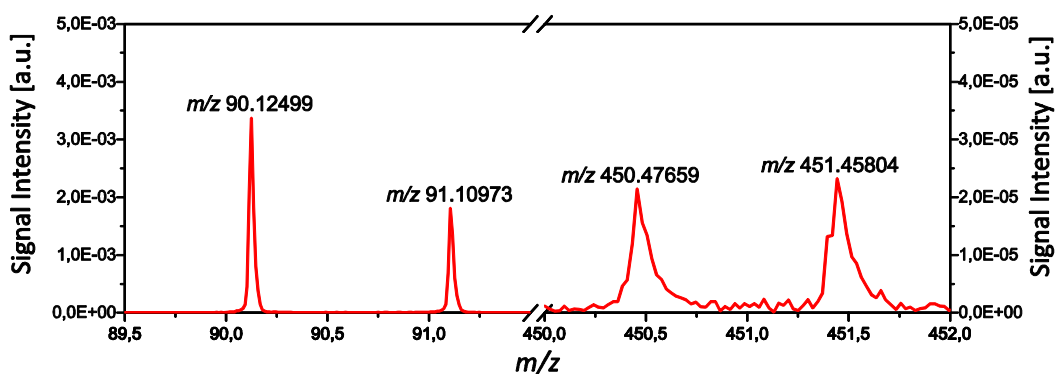


Fig. S2: Background spectrum of selected ions in lower and higher mass range, obtained by high-resolution time-of-flight mass spectrometry. Mass differences indicate the formation of ammonium water clusters.

Identification of NH_4^+ using ammonia addition

It has been shown for microwave plasmas that the addition of an aqueous ammonia solution can be adduced for an indirect identification of NH_4^+ formation in the plasma.⁵ Upon introduction of an ammonia solution into the interaction region, formation of a new series of clusters based on protonated ammonia clusters $[(\text{NH}_3)_n\text{H}]^+$ was observed. Here, an aqueous ammonia solution was deposited on the wooden handle of a cotton swab and introduced into the gap between plasma probe and inlet capillary at two different time intervals: 190 s – 240 s and 450 s – 500 s. The ion chronogram for the protonated water tetramer (m/z 37) and the proposed ammonium water adduct (m/z 36) decreases significantly whereas a new cluster signal with m/z 35, identified to be $[(\text{NH}_3)_2\text{H}]^+$, increases contemporary. These findings can be attributed to the individual amounts and characteristics of the formed primary ions. The proton affinity of water and ammonia are 691 kJ mol^{-1} and 854 kJ mol^{-1} , respectively.⁶ The exact m/z values for m/z 35, as well as its related water adducts, were also observed in the N_2 discharge indicating an active formation of ammonia in the plasma region. Via comparison of the individual voltage dependent characteristics and high-resolution mass spectrometry unambiguous identification has been achieved.

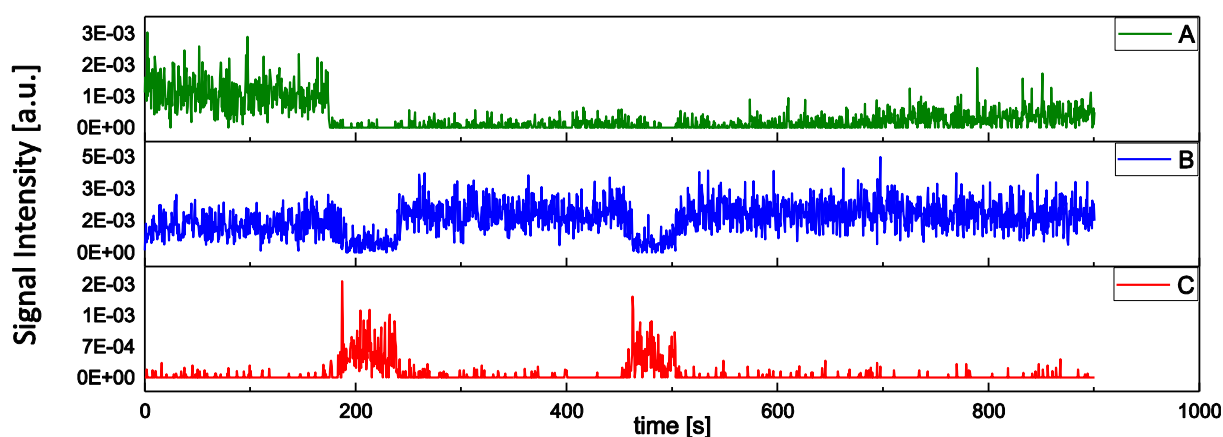
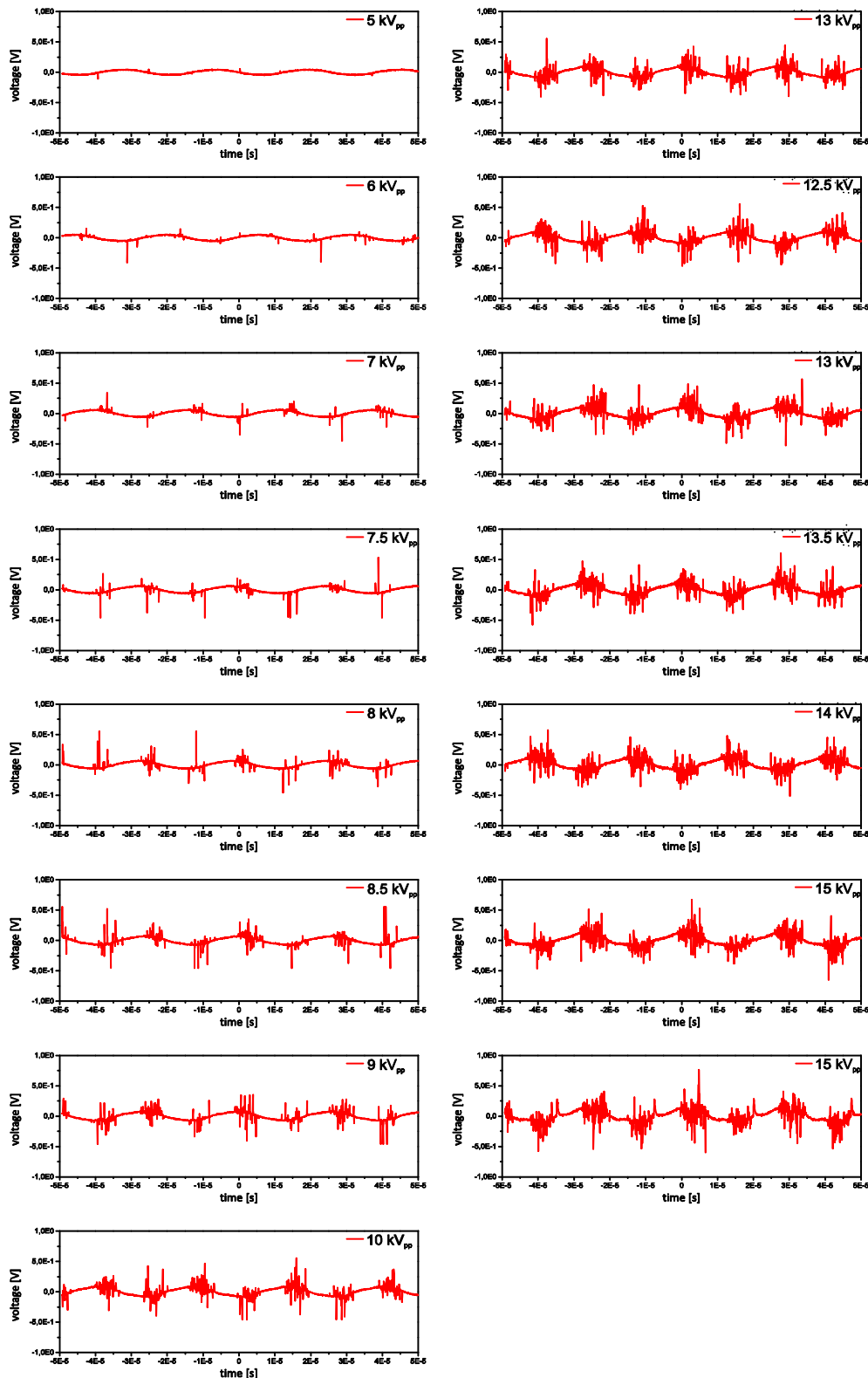


Fig. S3: Recorded extracted ion chronograms for m/z 37 (A), m/z 36 (B) and m/z 35 (C) using the He-DBD plasma in filamentary mode at $15 \text{ kV}_{\text{pp}}$.



76

Fig. S4: Detailed process of switching between the discussed operational modes: the homogeneous mode and the filamentary mode. Starting at lower voltages only strong, single, but regular distributed discharge events occur. As the applied voltage increases, a greater number of erratic current pulses were observed. If the applied input voltage became too high new events occur, indicating the capillary meltdown and direct arc formation (see last current/voltage profile).

82

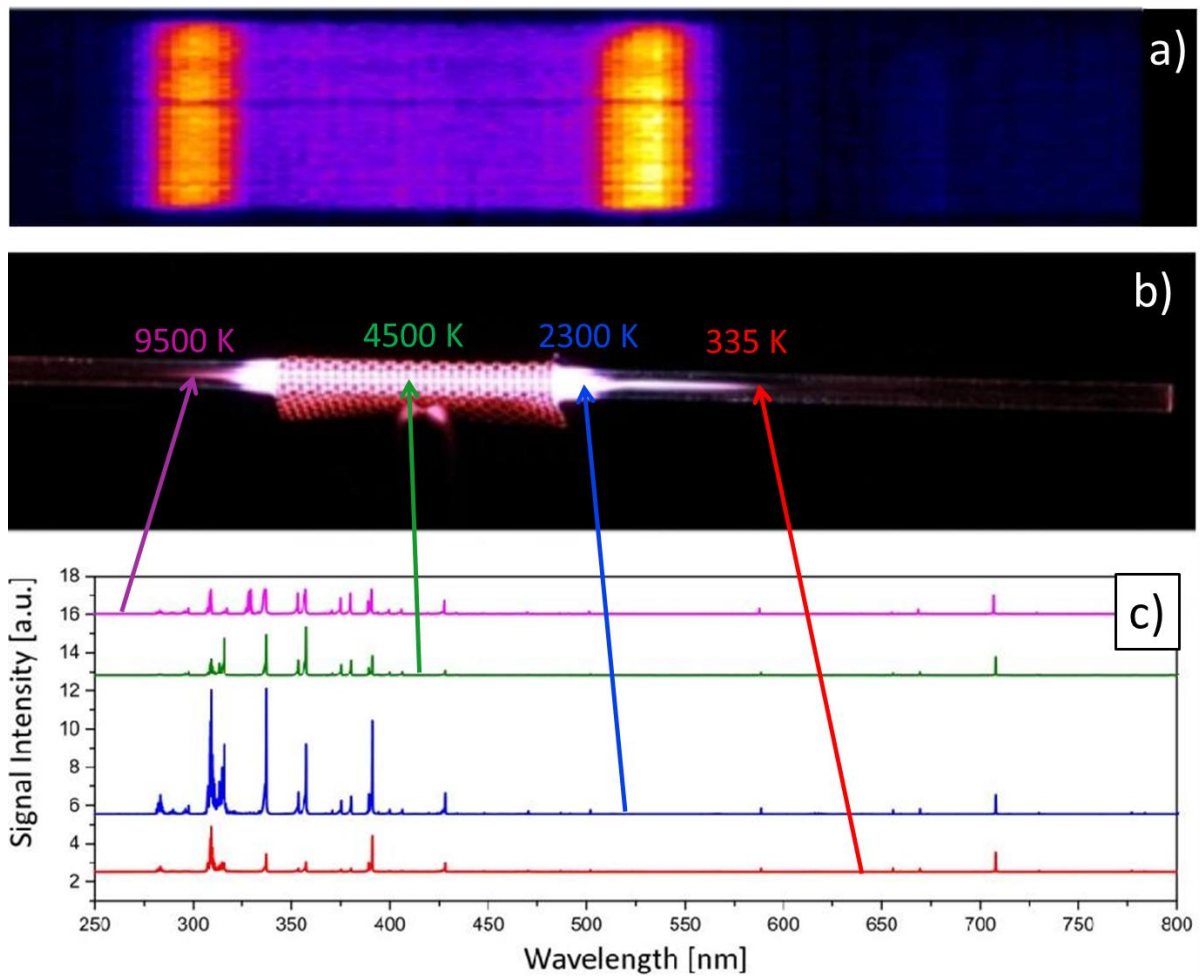


Fig. S5: Spectrally resolved spatial mapping of the used DBD torch. a) 2D distribution of spectral emission (exemplary shown here, emission originating from the $H\alpha$ -transition of the Balmer series at $\lambda = 656,28 \text{ nm}$). b) Photograph of the plasma for better orientation of the spatial scale/position (gas stream from left to right). c) selected UV/Vis emission spectra corresponding to the positions indicated by the arrows pointing towards Fig. S5 b). Spectra are vertically offset from each other for visualization aspects. Especially the signal intensities for N_2 , N_2^+ and OH showed the highest dependence on the spatial position in the plasma probe. Further, electron temperatures for individual positions were calculated via the Boltzmann populations of $H\alpha$ and $H\beta$.

Spectral lines:

He I (501.5 nm, 587.5 nm, 667.8 nm, 706.5 nm)

N_2^+ (band heads 391.4 nm, 427 nm)

N_2 (band heads 337 nm, 380 nm)

OH (band heads 281 nm, 306 nm)

O (777 nm)

101 **References**

- 102 1 J. T. Shelley, A. Stindt, J. Riedel and C. Engelhard, *J. Anal. At. Spectrom.*, 2014, **29**, 359–366.
- 103 2 F. J. Andrade, J. T. Shelley, W. C. Wetzels, M. R. Webb, G. Gamez, S. J. Ray and G. M. Hieftje,
104 *Anal. Chem.*, 2008, **80**, 2646–2653.
- 105 3 F. J. Andrade, J. T. Shelley, W. C. Wetzels, M. R. Webb, G. Gamez, S. J. Ray and G. M. Hieftje,
106 *Anal. Chem.*, 2008, **80**, 2654–2663.
- 107 4 E. Marotta and C. Paradisi, *J. Am. Soc. Mass Spectrom.*, 2009, **20**, 697–707.
- 108 5 T. Zhang, W. Zhou, W. Jin, J. Zhou, E. Handberg, Z. Zhu, H. Chen and Q. Jin, *J. Mass Spectrom.*,
109 2013, **48**, 669–676.
- 110 6 E. P. L. Hunter and S. G. Lias, *J. Phys. Chem. Ref. Data*, 1998, **27**, 413–656.

111